Chapter 13

Integration

In this book, we have considered many integrals in one and two dimensions. Some can be evaluated analytically, but many require numerical integration, or *quadrature*. In the Method of Moments, the accuracy of the solution depends strongly on the accuracy of the matrix elements, so a reliable and computationally efficient quadrature scheme is essential. This chapter considers several one-dimensional quadrature schemes and rules for integration over planar triangles.

The rules presented herein apply directly to smooth integrands. Singular and nearly singular integrals require additional treatment, such as singularity extraction, a suitable change of variables, or local subdivision. Increasing the number of quadrature points alone may be inefficient or unreliable in these cases.

13.1 One-Dimensional Integration

For the one-dimensional definite integral given by

$$I = \int_a^b f(x)\, dx \,, \tag{13.1}$$

a numerical quadrature rule generates an approximate solution using the sum

$$I = \int_a^b f(x)\, dx \approx \sum_{i=1}^{N} w(x_i) f(x_i) \,, \tag{13.2}$$

where the function $f(x)$ is evaluated at N unique locations x_i and multiplied by the quadrature weights $w(x_i)$. The weights and locations are dependent on the type and order of quadrature, often referred to as the quadrature *rule*. We will discuss several one-dimensional quadrature schemes in this section.

13.1.1 Centroidal Approximation

Some of the integrations in this book were evaluated using a centroidal approximation. This method simply evaluates the function once and assumes that its value is constant

within the limits of integration. The evaluation is typically done at the midpoint of the domain, resulting in an approximation given by

$$I = \int_a^b f(x)\, dx \approx (b-a) f\left([b+a]/2\right) \ . \tag{13.3}$$

This "one-point" quadrature rule is useful in cases where the integrand varies slowly, such as in computing the matrix elements between basis and testing function pairs that are far away from one another. In this case, the results from the centroidal rule often differ little from the results of a more accurate rule, but are much faster to compute. The error is often tolerable, since the magnitude of these elements is usually small compared to those closer to the matrix diagonal.

13.1.2 Rectangular Rule

The rectangular rule uses a stair-step approximation to $f(x)$ throughout the range of integration. We subdivide the interval $[a, b]$ into N small segments of equal length $h = (b-a)/N$ and compute the values $f(x_1)$, $f(x_2)$, ..., $f(x_N)$, as shown in Figure 13.1. The value of the integral within each segment is approximated as

$$\int_{x_i}^{x_{i+1}} f(x)\, dx \approx h f(x_i) \ . \tag{13.4}$$

Summing (13.4) across the entire interval, we derive the following expression for the rectangular rule

$$I = \int_a^b f(x)\, dx \approx h \sum_{n=1}^{N} f(x_n) + E_R \ , \tag{13.5}$$

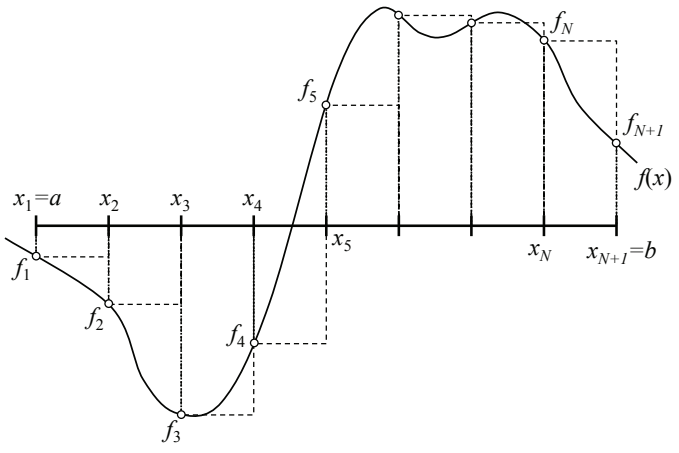


Figure 13.1: Rectangular (Stair-step) Approximation of $f(x)$

where E_R is the error. If $f''(x)$ is continuous within $[a, b]$, then the bound on the error is [1]

$$|E_R| \leq \frac{(b-a)h^2}{24} f''(\xi) \tag{13.6}$$

for some $\xi \in [a, b]$.

13.1.3 Trapezoidal Rule

The trapezoidal rule uses a piecewise linear approximation to $f(x)$ throughout the range of integration. We subdivide the interval $[a, b]$ into N small segments of equal length $h = (b-a)/N$ and compute the values $f(x_1)$, $f(x_2)$, ..., $f(x_N)$, $f(x_{N+1})$, as shown in Figure 13.2. The value of the integral within each segment is approximated as

$$\int_{x_i}^{x_{i+1}} f(x)\, dx \approx \frac{h}{2}\left[f_i + f_{i+1}\right]. \tag{13.7}$$

Summing (13.7) across the entire interval, we derive the following expression for the trapezoidal rule

$$I = \int_a^b f(x)\, dx \approx h\left[\frac{f_1}{2} + f_2 + \cdots + f_N + \frac{f_{N+1}}{2}\right] + E_T\ , \tag{13.8}$$

where E_T is the error. If $f''(x)$ is continuous within $[a, b]$, then the bound on the error is [1]

$$|E_T| \leq \frac{(b-a)h^2}{12} f''(\xi) \tag{13.9}$$

for some $\xi \in [a, b]$. If the result is not accurate enough, the number of segments can be doubled and the previous samples reused, requiring only N additional evaluations of $f(x)$ for the new rule. This process can be repeated as necessary until the desired accuracy is reached.

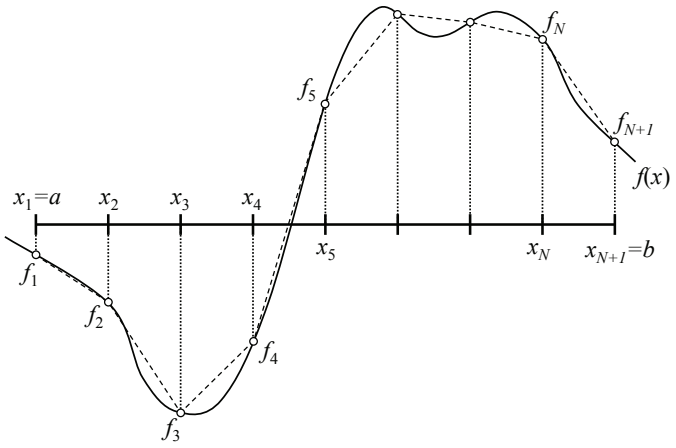


Figure 13.2: Piecewise Linear Approximation of $f(x)$

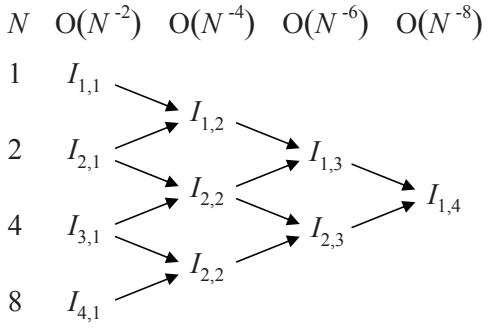


Figure 13.3: Hierarchy of Romberg Extrapolates

13.1.3.1 Romberg Integration

Repeated applications of the trapezoidal rule results in an error comprising even powers of $1/N$ [2], which can be written as

$$I = I_{n,1} + \frac{A}{N^2} + \frac{B}{N^4} + \frac{C}{N^6} + \cdots \; . \tag{13.10}$$

We note that the second-order term in the above decreases by a factor of four if we double the number of quadrature points. Using two applications of the rule, we can therefore write

$$I \approx I_{n,1} + \frac{K}{N^2} \tag{13.11}$$

and

$$I \approx I_{n+1,1} + \frac{K}{4N^2} \; . \tag{13.12}$$

If we solve the above two equations for K we can eliminate the second order term and improve the previous solution to at least an $O(N^{-4})$ error. Doing so yields

$$I \approx I_{n+1,2} = \frac{4}{3} I_{n+1,1} - \frac{1}{3} I_{n,1} \; , \tag{13.13}$$

which is a Richardson's extrapolation. Combining successive applications of the rule with higher orders of extrapolation can greatly increase the accuracy of the solution and is known as *Romberg integration*. In this method, higher-order extrapolates have the form

$$I_{n,m} = I_{n,m-1} + \frac{I_{n,m-1} - I_{n-1,m-1}}{4^{m-1} - 1} \; , \qquad 2 \leq m \leq n \; . \tag{13.14}$$

An example hierarchy of extrapolates is illustrated in Figure 13.3 for $n \leq 4$. Applying Romberg integration using this hierarchy requires the results of the trapezoidal rule using 1, 2, 4, and 8 segments.

13.1.4 Simpson's Rule

Simpson's rule approximates $f(x)$ by a series of quadratic polynomials, as shown in Figure 13.4. The interval $[a, b]$ is divided into N segments of equal length $h = (b - a)/N$, where $N \geq 2$ and even. Starting with the equation for a parabola

$$f(x) = Ax^2 + Bx + C \,, \tag{13.15}$$

we perform an integration over a two-segment interval $[-h, h]$, yielding

$$\int_{-h}^{h} \big(Ax^2 + Bx + C\big)dx = \left[A\frac{x^3}{3} + B\frac{x^2}{2} + Cx\right]\Bigg|_{-h}^{h} = \frac{h}{3}\big(2Ah^2 + 6C\big) \,. \tag{13.16}$$

Since the parabola passes through the points $(-h, f_1)$, $(0, f_2)$, and (h, f_3), we can compute the values

$$f_1 = Ah^2 - Bh + C \,, \tag{13.17}$$

$$f_2 = C \,, \tag{13.18}$$

and

$$f_3 = Ah^2 + Bh + C \,, \tag{13.19}$$

from which we obtain

$$2Ah^2 = f_1 + f_3 - 2f_2 \,. \tag{13.20}$$

Inserting (13.18) and (13.20) into (13.16) yields

$$\int_{-h}^{h} \big(Ax^2 + Bx + C\big)dx = \frac{h}{3}\Big[f_1 + 4f_2 + f_3\Big]. \tag{13.21}$$

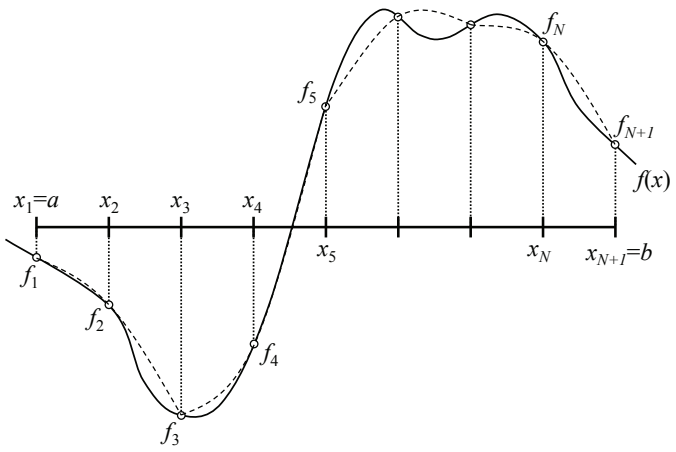


Figure 13.4: Piecewise Parabolic Approximation of $f(x)$

Summing (13.21) across the entire interval, we derive the following expression known as *Simpson's rule*

$$\int_a^b f(x)\,dx = \frac{h}{3}\left[f_1 + 4f_2 + 2f_3 + 4f_4 + \cdots + 2f_{N-1} + 4f_N + f_{N+1}\right] + E_S\ , \tag{13.22}$$

where E_S is the error. If $f^{(4)}(x)$ is continuous on $[a,b]$, then the bound on the error is [1]

$$|E_S| \leq \frac{b-a}{180}h^4 f^4(\xi) \tag{13.23}$$

for some $\xi \in [a,b]$. Note that the result of (13.21) is equal to that obtained by the extrapolation of the Trapezoidal rule in (13.13).

13.1.4.1 Adaptive Simpson's Rule

The Simpson's rule outlined thus far can be used in a recursive fashion similar to the Trapezoidal rule, where the number of segments is doubled and previous computations re-used. Writing the rule as

$$\int_a^b f(x)\,dx = S(a,b) + E_S\ , \tag{13.24}$$

and starting at the coarsest level (2 segments), we have

$$S(a,b) = \frac{b-a}{6}\left[f(a) + 4f\left(\frac{a+b}{2}\right) + f(b)\right] \tag{13.25}$$

and

$$E_S^{(1)} \leq \frac{b-a}{180}h^4 M\ , \tag{13.26}$$

resulting in

$$I^{(1)} = S(a,b) + E_S^{(1)}\ . \tag{13.27}$$

If we now divide the interval $[a,b]$ in half at $c = (a+b)/2$, we get

$$I^{(2)} = S(a,c) + S(c,b) + E_S^{(2)}\ . \tag{13.28}$$

The error is now

$$E_S^{(2)} \leq \frac{b-a}{180}\frac{h^4}{16}M = \frac{1}{16}E_S^{(1)}\ , \tag{13.29}$$

hence

$$S^{(2)} - S^{(1)} = E_S^{(2)} - E_S^{(1)} = -15E^2\ . \tag{13.30}$$

Using the above, we can stop the recursion once we reach a user-specified tolerance ϵ when

$$\frac{1}{15}\left|S^{(2)} - S^{(1)}\right| \leq \epsilon\ . \tag{13.31}$$

13.1.5 One-Dimensional Gaussian Quadrature

Using the trapezoidal or Simpson's rule, the interval $[a, b]$ is subdivided into equally spaced segments with fixed locations x_i. A more efficient integration rule can be developed if we allow the freedom to choose the optimal locations for integrating $f(x)$. Given the integral

$$\int_a^b W(x) f(x)\, dx\ , \tag{13.32}$$

for a positive weighting function $W(x)$ with the required finite moments, an N-point *Gaussian quadrature* integrates any polynomial $f(x)$ of degree at most $2N-1$ exactly. Its nodes are the roots of the degree-N orthogonal polynomial for the interval and weighting function, and its weights are chosen accordingly. The most commonly used Gaussian quadrature is the *Gauss-Legendre* quadrature, of the form

$$\int_{-1}^{1} f(x)\, dx \approx \sum_{i=1}^{N} w(x_i) f(x_i)\ , \tag{13.33}$$

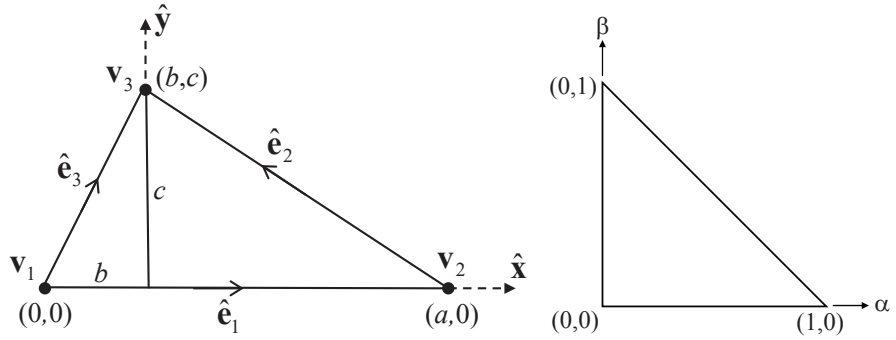
where $W(x) = 1$. The x_i for this rule are the roots of the Legendre polynomial of order N. The weights $w(x_i)$ are [3]

$$w(x_i) = \frac{2}{(1 - x_i^2)\big[P_N'(x_i)\big]^2}\ . \tag{13.34}$$

One common approach to computing an N-point Gauss-Legendre rule is to determine the locations of the zeros of $P_N(x)$ by Newton-Raphson iteration, and then compute the associated weights using (13.34). There are many short software routines for this task in numerical libraries and reference texts. Many of these retain the above range $[-1, 1]$, while some instead map to the range $[0, 1]$. To use the rule, a change of variable should be used to map the interval $[a, b]$ to $[-1, 1]$ or $[0, 1]$. Note that in this rule, the spacing between the quadrature locations is not constant. Therefore, previously computed values of $f(x)$ generally cannot be reused if the number of quadrature points is changed. In some cases, Simpson's rule may be the better choice.

13.2 Integration over Triangles

Many of the integrals in Chapter 8 and 12 are over triangular subdomains, and so efficient analytic and numerical integration techniques for triangular elements are also essential. In this section, we will consider these integrals in terms of *simplex coordinates*, also called *area coordinates* or *barycentric coordinates*. These coordinates comprise the transformation of a triangle of arbitrary shape to a canonical coordinate system. Analytic integrals are often easier to perform in simplex coordinates, and numerical quadrature rules are usually specified using them.



(a) Original Triangle (b) Transformed Triangle

Figure 13.5: Simplex Coordinates for a Triangle

13.2.1 Simplex Coordinates

To develop the transformation to simplex coordinates, consider the triangle T in Figure 13.5a, with vertices $\mathbf{v}_1$, $\mathbf{v}_2$, and $\mathbf{v}_3$, and edges given by

$$\mathbf{e}_1 = \mathbf{v}_2 - \mathbf{v}_1 \ , \qquad \mathbf{e}_2 = \mathbf{v}_3 - \mathbf{v}_2 \ , \qquad \mathbf{e}_3 = \mathbf{v}_3 - \mathbf{v}_1 \ . \tag{13.35}$$

Any point $\mathbf{r}$ within the triangle can be written as a weighted sum of the three vertices as

$$\mathbf{r} = \gamma\mathbf{v}_1 + \alpha\mathbf{v}_2 + \beta\mathbf{v}_3 \ , \tag{13.36}$$

where α, β, and γ are the simplex coordinates. These are subject to the constraint

$$\alpha + \beta + \gamma = 1 \ , \tag{13.37}$$

therefore,

$$\gamma = 1 - \alpha - \beta \ , \tag{13.38}$$

and

$$\mathbf{r} = (1 - \alpha - \beta)\mathbf{v}_1 + \alpha\mathbf{v}_2 + \beta\mathbf{v}_3 = \mathbf{v}_1 + \alpha\mathbf{e}_1 + \beta\mathbf{e}_3 \ . \tag{13.39}$$

Note that (13.36) has the form of a linear interpolation. Indeed, simplex coordinates will also allow us to perform a linear interpolation of a function $f(x, y)$ at points inside the triangle if its values are known at the vertices.

We can now transform an integral over the original triangle T to a new triangle T' in simplex coordinates, as shown in Figure 13.5b. The transformation is

$$\int_T f(\mathbf{r}) \, d\mathbf{r} = |J(\alpha,\beta)| \int_{T'} f(\alpha,\beta) \, d\alpha \, d\beta = 2A \int_0^1 \int_0^{1-\alpha} f(\alpha,\beta) \, d\beta \, d\alpha \ . \tag{13.40}$$

where the Jacobian $|J(\alpha, \beta)| = 2A$.

Given a point **r** inside a triangle, it is also desirable to obtain the simplex coordinates (α, β, γ). To do so, we first define $\hat{\boldsymbol{\rho}} = \mathbf{r} - \mathbf{v}_1$, and then use (13.39) to write

$$\alpha = \frac{|\hat{\boldsymbol{\rho}} \times \mathbf{e}_3|}{|\mathbf{e}_1 \times \mathbf{e}_3|} \tag{13.41}$$

and

$$\beta = \frac{|\mathbf{e}_1 \times \hat{\boldsymbol{\rho}}|}{|\mathbf{e}_1 \times \mathbf{e}_3|} \ . \tag{13.42}$$

13.2.2 Radiation Integrals with a Constant Source

We now consider radiation integrals having a constant-valued integrand, written as

$$I = \int e^{j\mathbf{s}\cdot\mathbf{r}'} \, d\mathbf{r}' \ , \tag{13.43}$$

which is also the phase integral from (12.70) with $\mathbf{s} = k_0(\hat{\mathbf{r}}^i + \hat{\mathbf{r}}^s)$. We will evaluate this integral for the triangle T in Figure 13.5a, where after transforming the integral to simplex coordinates and using (13.40), it can be written as

$$I = \int e^{j\mathbf{s}\cdot\mathbf{r}'} \, d\mathbf{r}' = 2A \int_0^1 \int_0^{1-\alpha} e^{j\mathbf{s}\cdot\mathbf{r}'(\alpha,\beta)} d\beta \, d\alpha \ . \tag{13.44}$$

where the area A of the triangle is given by

$$A = \frac{1}{2}|\mathbf{e}_1 \times \mathbf{e}_3| \ . \tag{13.45}$$

Substituting **r** from (13.39) into (13.44) allows us to then write

$$I = 2Ae^{j\mathbf{s}\cdot\mathbf{v}_1} \int_0^1 \int_0^{1-\alpha} e^{j\mathbf{s}\cdot\mathbf{e}_1\alpha} e^{j\mathbf{s}\cdot\mathbf{e}_3\beta} d\beta \, d\alpha \ , \tag{13.46}$$

or

$$I = 2Ae^{js_1} \int_0^1 e^{js_2\alpha} \int_0^{1-\alpha} e^{js_3\beta} d\beta \, d\alpha \ , \tag{13.47}$$

where

$$s_1 = \mathbf{s}\cdot\mathbf{v}_1 \ , \qquad s_2 = \mathbf{s}\cdot\mathbf{e}_1 \ , \qquad s_3 = \mathbf{s}\cdot\mathbf{e}_3 \ . \tag{13.48}$$

Evaluating the integral with respect to β yields

$$I = 2Ae^{js_1} \int_0^1 e^{js_2\alpha} \left(\frac{e^{js_3(1-\alpha)}}{js_3} - \frac{1}{js_3} \right) d\alpha \ , \tag{13.49}$$

which can be rewritten as

$$I = 2A\frac{e^{js_1}}{js_3} \int_0^1 \left(e^{js_3} e^{j\alpha(s_2-s_3)} - e^{j\alpha s_2} \right) d\alpha \ . \tag{13.50}$$

Integrating over α yields

$$I = 2A\frac{e^{js_1}}{js_3}\left(\frac{e^{js_2}}{j(s_2-s_3)} - \frac{e^{js_2}}{js_2} - \frac{e^{js_3}}{j(s_2-s_3)} + \frac{1}{js_2}\right), \tag{13.51}$$

and after some tedious but straightforward algebra, we finally obtain

$$I = 2A\frac{e^{js_1}}{(s_2-s_3)}\left(\frac{1-e^{js_2}}{s_2} - \frac{1-e^{js_3}}{s_3}\right). \tag{13.52}$$

13.2.2.0.1 Special Cases

There are several cases where (13.52) is not valid. The first occurs when **s** is normal to the triangle, thus $s_2 = s_3 = 0$. In this case, (13.43) is simply

$$I = Ae^{js_1}\ . \tag{13.53}$$

The second occurs when **s** is not normal to the triangle, and $\mathbf{s}\cdot\mathbf{e}_1 = \mathbf{s}\cdot\mathbf{e}_3$, or $s_2 = s_3$. In this case, we re-evaluate (13.50) by setting $s_2 = s_3 = s$, which yields

$$I = -2A\frac{e^{js_1}}{s^2}\left[1 + e^{js}(js-1)\right]\ . \tag{13.54}$$

The last occurs when **s** is normal to $\mathbf{e}_1$ or $\mathbf{e}_3$, and so either $s_2 = 0$ or $s_3 = 0$. In this case, the first or second term inside the parenthesis in (13.52), respectively, evaluates to $-j$.

13.2.3 Radiation Integrals with a Linear Source

Next we consider a radiation integral with a linearly varying source, such as the RWG function described in Section 8.2. This integral can be written as

$$\mathbf{I} = \int_T \boldsymbol{\rho}(\mathbf{r}')e^{j\mathbf{s}\cdot\mathbf{r}'}\,d\mathbf{r}'\ , \tag{13.55}$$

where the source function is

$$\boldsymbol{\rho}(\mathbf{r}') = \mathbf{r}' - \mathbf{v}_1\ . \tag{13.56}$$

This corresponds to the RWG function defined on the edge opposite vertex $\mathbf{v}_1$ on triangle T in Figure 13.5a. After transforming the integral to simplex coordinates and using (13.40), it can be written as

$$\mathbf{I} = 2A\int_0^1\int_0^{1-\alpha}\boldsymbol{\rho}(\mathbf{r}')e^{j\mathbf{s}\cdot\mathbf{r}'(\alpha,\beta)}d\beta\,d\alpha\ , \tag{13.57}$$

and expanding $\mathbf{r}'(\alpha,\beta)$ following (13.39), we can write the above as

$$\mathbf{I} = 2Ae^{js_1}\int_0^1\int_0^{1-\alpha}(\alpha\mathbf{e}_1 + \beta\mathbf{e}_3)e^{js_2\alpha}e^{js_3\beta}d\beta\,d\alpha\ , \tag{13.58}$$

where s_1, s_2, and s_3 are defined in (13.48).

13.2.3.1 General Case

For the general case, (13.58) evaluates to

$$\mathbf{I} = -\frac{C}{s_3}\left[e^{js_2}\left(\frac{1-j(s_2-s_3)}{(s_2-s_3)^2}+\frac{js_2-1}{s_2^2}\right)-\frac{e^{js_3}}{(s_2-s_3)^2}+\frac{1}{s_2^2}\right]\mathbf{e}_1$$
$$-\frac{C}{s_2}\left[e^{js_3}\left(\frac{1-j(s_3-s_2)}{(s_3-s_2)^2}+\frac{js_3-1}{s_3^2}\right)-\frac{e^{js_2}}{(s_3-s_2)^2}+\frac{1}{s_3^2}\right]\mathbf{e}_3\ , \tag{13.59}$$

or

$$\mathbf{I} = \frac{C}{s_3}\left[B(s_2)-e^{-js_3}B(s_2-s_3)\right]\mathbf{e}_1+\frac{C}{s_2}\left[B(s_3)-e^{-js_2}B(s_3-s_2)\right]\mathbf{e}_3 \tag{13.60}$$

where

$$B(s) = \frac{e^{js}(1-js)-1}{s^2} \tag{13.61}$$

and

$$C = j2Ae^{js_1}. \tag{13.62}$$

As in Section 13.2.2, this expression has singularities when **s** is perpendicular to any of the three edges. Therefore, we must also consider the special cases.

13.2.3.2 Special Cases

When **s** is perpendicular to $\mathbf{e}_1$ ($s_2 = 0$), we can write (13.58) as

$$\mathbf{I} = 2Ae^{js_1}\int_0^1\int_0^{1-\alpha}(\alpha\mathbf{e}_1+\beta\mathbf{e}_3)e^{js_3\beta}d\beta\ d\alpha\ , \tag{13.63}$$

which evaluates to

$$\mathbf{I} = C\left[\frac{-1-js_3}{s_3^3}+\frac{1}{2s_3}+\frac{e^{js_3}}{s_3^3}\right]\mathbf{e}_1+C\left[e^{js_3}\left(\frac{js_3-2}{s_3^3}\right)+\frac{2}{s_3^3}+\frac{j}{s_3^2}\right]\mathbf{e}_3\ . \tag{13.64}$$

When **s** is perpendicular to $\mathbf{e}_3$ ($s_3 = 0$), we can write (13.58) as

$$\mathbf{I} = 2Ae^{js_1}\int_0^1\int_0^{1-\alpha}(\alpha\mathbf{e}_1+\beta\mathbf{e}_3)e^{js_2\alpha}d\beta\ d\alpha\ , \tag{13.65}$$

which evaluates to

$$\mathbf{I} = C\left[e^{js_2}\left(\frac{js_2-2}{s_2^3}\right)+\frac{2}{s_2^3}+\frac{j}{s_2^2}\right]\mathbf{e}_1+C\left[\frac{-1-js_2}{s_2^3}+\frac{1}{2s_2}+\frac{e^{js_2}}{s_2^3}\right]\mathbf{e}_3\ . \tag{13.66}$$

When $s_2 = s_3 = s, s \neq 0$, we can write (13.58) as

$$\mathbf{I} = 2Ae^{js_1}\int_0^1\int_0^{1-\alpha}(\alpha\mathbf{e}_1+\beta\mathbf{e}_3)e^{js(\alpha+\beta)}d\beta\ d\alpha\ , \tag{13.67}$$

which evaluates to

$$\mathbf{I} = C\left[e^{js}\left(\frac{1}{s^3}-\frac{1}{2s}-\frac{j}{s^2}\right)-\frac{1}{s^3}\right]\left[\mathbf{e}_1+\mathbf{e}_3\right]. \tag{13.68}$$

When **s** is normal to the triangle, 13.58 becomes

$$\mathbf{I} = 2Ae^{j\mathbf{s}\cdot\mathbf{v}_1} \int_0^1 \int_0^{1-\alpha} (\alpha\mathbf{e}_1 + \beta\mathbf{e}_3) d\beta \; d\alpha \; , \tag{13.69}$$

which evaluates to

$$\mathbf{I} = \frac{A}{3} e^{js_1} \big(\mathbf{e}_1 + \mathbf{e}_3\big). \tag{13.70}$$

13.2.4 Gaussian Quadrature on Triangles

The most commonly referenced Gauss-Legendre locations and weights for triangles are the symmetric quadrature rules presented in [4]. In this reference are tables varying from degrees 1 up to 20 (79 quadrature points). Tables for orders 2–5 are reproduced in Figures 13.1, 13.2, 13.3, and 13.4, respectively. The weights in these tables are normalized with respect to triangle area, i.e.

$$\int_S f(x,y)\; dx\; dy \approx A \sum_{i=1}^{N} w(\alpha_i, \beta_i) f(\alpha_i, \beta_i) \; . \tag{13.71}$$

It is this author's experience that the three-point quadrature rules work well for the example problems presented in Chapters 8–11.

Table 13.1: Three-Point Quadrature Rule ($n = 2$)

i	α	β	γ	w
1	0.66666667	0.16666667	0.16666667	0.33333333
2	0.16666667	0.66666667	0.16666667	0.33333333
3	0.16666667	0.16666667	0.66666667	0.33333333

Table 13.2: Four-Point Quadrature Rule ($n = 3$)

i	α	β	γ	w
1	0.33333333	0.33333333	0.33333333	-0.56250000
2	0.60000000	0.20000000	0.20000000	0.52083333
3	0.20000000	0.60000000	0.20000000	0.52083333
4	0.20000000	0.20000000	0.60000000	0.52083333

13.2.4.1 Comparison with Analytic Solution

The formulas presented in Sections 13.2.3.1 and 13.2.3.2 are advantageous as they are analytic solutions which are valid at all frequencies. By comparison, an accurate numerical quadrature requires an increasing number of integration points as the electrical size of the triangle increases, which is undesirable. Let us compare the analytic solution to the radiation integral with linear source (13.58), summarized in (13.59), to

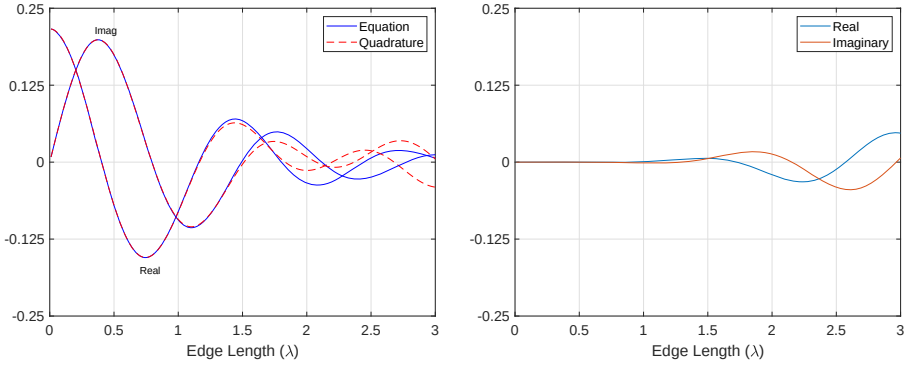
Table 13.3: Six-Point Quadrature Rule ($n = 4$)

i	α	β	γ	w
1	0.10810301	0.44594849	0.44594849	0.22338158
2	0.44594849	0.10810301	0.44594849	0.22338158
3	0.44594849	0.44594849	0.10810301	0.22338158
4	0.81684757	0.09157621	0.09157621	0.10995174
5	0.09157621	0.81684757	0.09157621	0.10995174
6	0.09157621	0.09157621	0.81684757	0.10995174

Table 13.4: Seven-Point Quadrature Rule ($n = 5$)

i	α	β	γ	w
1	0.33333333	0.33333333	0.33333333	0.22500000
2	0.05971587	0.47014206	0.47014206	0.13239415
3	0.47014206	0.05971587	0.47014206	0.13239415
4	0.47014206	0.47014206	0.05971587	0.13239415
5	0.79742698	0.10128650	0.10128650	0.12593918
6	0.10128650	0.79742698	0.10128650	0.12593918
7	0.10128650	0.10128650	0.79742698	0.12593918

that obtained using a 7-point Gaussian quadrature rule (Table 13.4). The source triangle is equilateral and lies in the xy plane with vertices $\mathbf{v}_1 = (0, 0)$, $\mathbf{v}_2 = (l, 0)$, and $\mathbf{v}_3 = (l/2, l\sqrt{3}/2)$. The direction of radiation is along the spherical angles $(\theta, \phi) = (\pi/2, \pi/4)$. In Figure 13.6a we compare the magnitude of the x component of (13.59) versus the triangle edge length l in wavelengths. In Figure 13.6b we plot the difference between the results. We see that the analytical and numerical results compare very well to just over $l = 1\lambda$, at which point the numerical results start to diverge.



(a) x Component (b) x Difference

Figure 13.6: Linear Source Radiation Integral: Equation vs. Quadrature

References

[1] G. Thomas and R. Finney, *Calculus and Analytic Geometry*. Addison-Wesley, 1992.

[2] A. F. Peterson, S. L. Ray, and R. Mittra, *Computational Methods for Electromagnetics*. IEEE Press, 1998.

[3] W. H. Press, B. P. Flannery, S. A. Teukolsky, and W. T. Vetterling, *Numerical Recipes in C : The Art of Scientific Computing*. Cambridge University Press, 1992.

[4] D. Dunavant, "High degree efficient symmetrical Gaussian quadrature rules for the triangle," *Internat. J. Numer. Methods Engrg.*, vol. 21, pp. 1129–1148, 1985.